A MODIFIED NORMALIZATION METHOD FOR DETERMINING FRACTURE TOUGHNESS OF STEEL

Hui Gao, Weigang Wang Yanlin Wang, Bohua Zhang and Chun-Qing Li*
School of Engineering, RMIT University, Melbourne, 3001, Australia

ABSTRACT

Normalization method is a practical method for determining the *J*-R curves and fracture toughness of steels. There is some concern, however, about the performance of this method on steels with small strain hardening exponent and yield strength due mainly to the assumption of infinite strain hardening exponent (n). This paper intends to analytically modify the normalization method by removing this assumption and incorporating the strain hardening in calculating the blunting corrected crack length. This modification enables the normalization method to be applied to steels with small strain hardening exponent and yield strength. Experiments are undertaken to prove the underperformance of the normalization method for steels with small strain hardening exponent and yield strength and to verify the modified normalization method (CNM). A comparison of fracture toughness determined by CNM with that by the unloading compliance method and normalization method corroborates the improved accuracy of the developed CNM. It is found in the paper that the developed CNM performs very well for materials with small strain hardening exponent and yield strength and performs better for specimens with smaller thickness and in accordance with all standards. The paper concludes that the developed CNM overcomes the deficiency of the normalization method for steels with small strain hardening exponent and yield strength.

KEYWORDS

Normalization method; Fracture toughness; *J*-resistance curve; Strain hardening exponent; Blunting corrected crack length.

* Corresponding author, Professor Chun-Qing Li, email: chunqing.li@rmit.edu.au

Nomenclature

a_0 = initial crack length

a_{bi} = blunting corrected crack length at the *i*th loading point

a_{bni} = strain hardening corrected blunting crack length

B = specimen thickness

d_n = dimensionless constant

E = Young's modulus

J = J-integral

$J_{0.2}$ = fracture toughness determined in accordance with BS 7448-4:1997

$J_{0.2BL}$ = fracture toughness determined in accordance with ISO 12135:2016 (E)

J_{Ic} = fracture toughness determined in accordance with ASTM E1820-18

n = strain hardening exponent

P_{Ni} = i^{th} normalized load

P_{Nni} = strain hardening corrected i^{th} normalized load

W = specimen width

α = dimensionless constant in Ramberg-Osgood equation

$\Delta a_{0.2b}$ = difference in crack length corresponding to $J_{0.2}$

45 Δa_{bi} = blunted crack advance

46 Δa_{bni} = difference in crack length because of the n infinity assumption

47 δ_i = crack tip opening displacement (CTOD)

48 η_{pl} = plastic geometry factor

49 σ_0 = reference stress that is usually equal to the yield strength ($\sigma_0 = \sigma_{\mathrm{YS}}$)

50 $\varepsilon_0 = \sigma_0/E$

51 σ_{TS} = ultimate tensile strength

52 σ_{Y} = effective yield strength

53 σ_{YS} = yield strength

54 **Abbreviations**

55	CMOD	crack mouth opening displacement
56	CNM	blunting crack length corrected normalization method
57	*J*-R	*J*-integral-resistance
58	NM	normalization method
59	*P*-*V*	load-CMOD
60	SE(B)	single edge notched specimen
61	UC	unloading compliance method

1. INTRODUCTION

Fracture toughness represents the ability of a material to resist fracture. It is an important mechanical property of metals used in engineering design and failure assessment of metal structures. Fracture toughness is usually determined through laboratory tests. However, tests on fracture toughness can be difficult because of the difficulty in measuring the crack extension in specimens. A most widely used and reliable method for determining the crack extension is the unloading compliance (UC) method proposed by Clarke et al. [1]. This method has been adopted by various standards, such as ASTM E1820 [2], BS 7448-4 [3] and ISO 12135[4]. The principle of the UC method is to relate the crack extension to the compliance of the specimen. However, tests with the unloading-reloading process of the UC method are tedious and time-consuming, compared with the monotonic loading tests. It is also difficult to apply unloading-reloading in harsh conditions, such as high loading rate, high temperature, corrosion, or other aggressive environments. As such, a normalization method (NM) was developed by Herrera and Landes [5], based on the key-curve method [6] and the principle of load separation [7-10].

The normalization method (NM) directly uses the monotonic load-displacement or load-crack mouth opening displacement (CMOD) record to determine the *J*-Resistance (*J*-R) curve for the specimen without the unloading-reloading process [11-14]. In NM, a calibration function needs to be established to determine the instantaneous crack length corresponding to the load and displacement test data. Various forms of calibration functions have been developed. Herrera and Landes [5] proposed a power-law calibration function in 1988. The calibration function is described in terms of two separated parts of elastic and plastic displacements. The relationship between the plastic part of the displacement and load is expressed in terms of a power function with constant coefficients and exponent [7-9]. Herrera and Landes [5] applied the power-law calibration function to various types of steel and found that it worked well.

In 1990, Herrera and Landes [11] found that the developed power-law calibration function did not work well for materials whose stress-strain relationship does not follow a power law, such as 304 stainless steel. They then developed a combined calibration function of power-law and straight line instead of the single power-law calibration function. After being applied to a variety of materials, the developed combined calibration function was verified [11]. In the meantime, Orange [12] and Landes et al. [14] developed a three-parameter *LMN* function. This new form of the function contains three unknown fitting constants (*L, M, N*), which can be determined for all specimen geometries, based on the work of Sharobeam and Landes [10]. After being applied to various types of steels, such as A508 steel and HSLA steel, the *J*-R curve determined using the *LMN* function agrees well with that using the unloading compliance method. With further improvement, the three-parameter *LMN* function was finally incorporated in the ASTM E1820-18 Annex 15 [2] as the calibration function of the normalization method. The normalization method was also verified by Scibetta et al. [15] in 2006 using numerical simulations, and with different materials, including steels [16-18], alloys [19] and polymers [20-24]. Furthermore, Dubey et al. [25] successfully used the normalization method to determine the fracture toughness of un-irradiated Zircaloy-2 pressure tubes under different temperatures.

The performance in terms of accuracy of the normalization method (NM) for a range of steels has been investigated by various researchers with different specimens materials [26-33]. They used UC as the benchmark to evaluate the performance of NM because UC is popular and usually assumed to be reliable. Their test results show that a large difference exists in fracture toughness as determined by UC and NM. For example, Dzugan and Viehrig [26] showed that the difference in fracture toughness of SFA steel between these two methods can be as large as 17%. Zhu and Joyce [27] found that the deviation in the mean fracture toughness of HY80 steel with 12 specimens, as determined by UC and NM, was around 10%. For HSLA steel, Menezes

et al. [32] found that the average difference in fracture toughness J_{Ic} with 2 specimens obtained by UC and NM was 9%.

An examination of test results in these references [26-33] shows that the degree of difference in fracture toughness depends on the mechanical properties of the tested materials. For SUS 316L steel, A285 carbon steel, and THS steel, the *J*-R curves and fracture toughness determined by the normalization method, the unloading compliance method and the electric potential method are almost identical [26, 29, 32]. However, for 10CrMo9-10 steel, HY80 steel, X80 pipeline steel and HSLA steel, the *J*-R curves and fracture toughness determined by the normalization method show noticeable deviation from those by the unloading compliance method [26-28, 32]. The degree of differences for different seels raises concerns about the accuracy of the normalization method, which may cause problems in practices, in particular, in structural design and safety assessment. This concern gives rise to the need to investigate the underlying factors that affect the accuracy of the normalization method, based on which a new or improved method can be developed.

Gao et al. [33] conducted a series of tests on fracture toughness with different types of steel. They observed that the performance or accuracy of the normalization method (NM) depends on the mechanical properties of the material. The *J*-R curves and fracture toughness of steels with small strain hardening exponent and yield strength, such as G250 steel, can be underestimated by NM. This underestimation is mainly attributed to the assumption in NM that the strain hardening exponent (n) is infinity in calculating the blunting corrected crack length (a_{bi}). As strain hardening exponent is not infinity for most steels if not all, it is therefore necessary to incorporate the strain hardening in the normalization method. This is particularly necessary for steels with small strain hardening exponent and yield strength, such as G250 steel. It is with this regard that the present paper is in order.

The intention of this paper is to analytically modify the normalization method by incorporating the strain hardening in calculating the blunting corrected crack length (a_{bi}). This modification enables the normalization method to be applied to steels with small strain hardening exponent and yield strength. The modified method is hereafter referred to as blunting crack length corrected normalization method, donated as CNM. Experiments were undertaken to prove that the mechanical properties of steel do affect the performance of the normalization method, and to verify the accuracy of the developed CNM. The fracture toughness determined by CNM following different standards is compared with that determined by UC and NM, and the results show the improved accuracy of the normalization method after it is corrected. The factors that affect the performance of the developed CNM are also investigated.

2. THE MODIFIED NORMALIZATION METHOD

A core advantage of the normalization method is that it can estimate the crack length without the unloading-reloading process during the test. Originally, the normalization method (NM) directly uses the load vs. load-line displacement (LLD) curve together with the final crack length to determine the *J*-R curve. However, because the measurement of LLD is less accurate and more difficult due to such factors as specimen load point indentions, transducer mounting difficulties and load train deflections or a combination of these factors [34], more accurate measurement of crack mouth opening displacement (CMOD) becomes desirable in NM. As a result, a load vs. CMOD (*P*-*V*) curve to determine *J*-R curves has been accepted. Scibetta et al. [15] used numerical simulations to prove that all equations of the LLD-based NM are still valid when load vs. CMOD curves were used. They found that the difference in J_{Ic} determined by LLD and CMOD with the same equations was less than ±2%. In addition, their simulation results were almost identical to the test results carried out by Lucon et al. [35]. Thus, the load

158 vs. CMOD curves have been verified for NM and used by a number of researchers to achieve
159 their research objectives [32, 33, 36-38].

160 In normalization method, the following procedure is used to determine the crack extension
161 according to ASTM E1820 Annex 15 [2]. At first, each load P_i in the range from 0 to the
162 maximum load (excluding the maximum load) is normalized using the following expression [2]

163 $$P_{Ni} = \frac{P_i}{WB\left(1-\frac{a_{bi}}{W}\right)^{\eta_{pl}}} \quad (1)$$

164 where P_{Ni} is the normalized load and i refers to the i^{th} loading; W is the specimen width; B is
165 the specimen thickness; η_{pl} is a plastic geometry factor that is given in ASTM E1820 Annex 1
166 [2] if CMOD is used for three-point bending specimens; and a_{bi} is the blunting corrected crack
167 length at the i^{th} loading point, given as follows

168 $$a_{bi} = a_0 + \Delta a_{bi} \quad (2)$$

169 where a_0 is the initial crack length and Δa_{bi} is the blunted crack advance.

170 The blunting corrected crack length (a_{bi}) is a key parameter in the normalization method, but
171 the equation for calculating the blunted crack advance, Δa_{bi}, is different in different standards.
172 In ASTM E1820 [2], Δa_{bi} is determined as follows

173 $$\Delta a_{bi} = \frac{J_i}{2\sigma_Y} \quad (3)$$

174 and in BS 7448-4 [3], Δa_{bi} is determined as follows

175 $$\Delta a_{bi} = \frac{J_i}{3.75\sigma_{TS}} \quad (4)$$

where J_i is the J-integral, σ_Y is the effective yield strength, which is taken as the average of yield strength (σ_{YS}) and ultimate tensile strength (σ_{TS}).

In addition to the above two equations for Δa_{bi}, another equation was presented in Zhou et al. [13]. Zhou et al. [13] are the first to propose the assumed artificial blunting behaviour and blunting corrected crack length equation to improve the accuracy of the normalization method. In Zhou et al. [13], the blunted crack advance Δa_{bi} is determined as follows

$$\Delta a_{bi} = \frac{J_i}{2\sigma_Y} \text{ or } \Delta a_{bi} = \frac{J_i}{2\sigma_{YS}} \tag{5}$$

It can be seen that these three equations are all different in determining Δa_{bi}. Therefore, it is necessary to revisit the original definition of Δa_{bi} to develop an accurate equation for it. Landes and Begley [39] shown a stretch zone between the initial crack tip and the point of material separation. The stretch zone is formed by the crack tip blunting, the length of which, denoted as Δa_{bi}, is shown in Fig. 1.

Figure 1 Blunted crack length ($a_{bi} = a_0 + \Delta a_{bi}$) [40]

The length of this stretch zone is approximated to be half of the crack tip opening displacement (δ_i) with $\delta_i \approx \frac{J_i}{\sigma_{YS}}$. Moreover, Anderson [40] and Landes [41] also suggested that $\Delta a_{bi} = \frac{\delta_i}{2}$, as shown in Fig. 1.

Landes and Begley [39] proposed that σ_{YS} is used to calculate the length of stretch zone and $2\sigma_{\mathrm{Y}}$ was chosen as the slope of blunting line. In ASTM E1820 and many other literatures [14, 26-30], σ_{Y} is used for determining the blunted crack advance Δa_{bi}. As stated in Landes and Begley [39], the purpose of the blunting line is to determine fracture toughness, J_{Ic}, not the blunting corrected crack length a_{bi}. The value of Δa_{bi} shall still be equal to half of crack tip

opening displacement (i.e., $\frac{\delta_i}{2}$). Anderson [40] suggested that σ_{YS} should be used instead of σ_Y to calculate δ_i and Δa_{bi}. Therefore, the blunting corrected crack length a_{bi} can be calculated accurately according to [39-41] as follows

$$a_{bi} = a_0 + \frac{\delta_i}{2} = \frac{J_i}{2\sigma_{YS}} \tag{6a}$$

Moreover, according to Anderson [40] and Shih [42], the crack tip opening displacement (CTOD) δ_i can be determined as follows

$$\delta_i = \frac{d_n J_i}{\sigma_0} \tag{6b}$$

where σ_0 is the reference stress that is usually equal to the yield strength (i.e., $\sigma_0 = \sigma_{YS}$); d_n is a dimensionless constant that was firstly proposed by Shih in 1981 [42] to correlate *J*-integral with CTOD. Fig. 2 shows how d_n is determined for both plane stress and strain conditions, when α = 1, where α is a dimensionless constant of Ramberg-Osgood material model [43], expressed as follows

$$\frac{\varepsilon}{\varepsilon_0} = \frac{\sigma}{\sigma_0} + \alpha\left(\frac{\sigma}{\sigma_0}\right)^n \tag{6c}$$

where $\varepsilon_0 = \sigma_0/E$ and n is the strain hardening exponent. When $\alpha \neq 1$, d_n determined in Fig. 2 should be multiplied by $\alpha^{1/n}$.

It should be noted that there are two definitions for strain hardening exponent, which are almost reciprocal. As the HRR theory is developed using the Ramberg-Osgood equation i.e., Eq. (6c) [40]. The strain hardening exponent used in this study is based on the Ramberg-Osgood equation with $n \geq 1$. It also should be noted that Eq. (6b) is based on the HRR theory which

does not account for large geometry changes at the crack tip. The stresses predicted by the HRR theory seems inaccurate for $r < 2\,\delta$ (r is the distance to the crack tip). Shih [42] used the HRR theory to determine the displacements well within the large strain region [40] which then were verified by the finite element analyses. The results in Shih [42] show that the relationship between *J*-integral and CTOD for the large strain region is in general agreement with Eq. (6b). Thus the displacement fields predicted from the HRR theory are reasonably accurate, despite the large plastic strains at the crack tip [40]. As such, d_n is valid for the deformation behavior of metallic materials used in this study.

Figure 2 Value of d_n for plane stress (a) and plane strain (b) conditions with α=1 [40, 42]

It can be seen from Fig. 2 that d_n highly depends on the strain hardening exponent (n), and moderately depends on the ratio of σ_0/E. For plane strain condition, d_n is approximately 0.78 for non-hardening material ($n = \infty$). If d_n = 1, it is for an assumption of non-hardening material ($n = \infty$) in the plane-stress condition [40]. It can also be seen from Fig. 2 that if strain hardening exponent is assumed to be infinity, the effect of yield stress on d_n is also eliminated. Clearly, for strain hardening materials, the parameter d_n should be determined by both strain hardening exponent (n) and yield strength (σ_0/E) of the material. Although d_n has been proposed for a while [37], it has not been employed to correct the blunted crack advance (Δa_{bi}), which can improve the accuracy of the normalization method.

The equation for determining blunting corrected crack length a_{bi} used in ASTM E1820 and many other literatures (see references above) is under the assumption of d_n = 1 for both hardening and non-hardening materials, which results in an overestimation of a_{bi} for hardening materials, whose d_n is $0 < d_n \leq 1$ [33]. Therefore, the parameter d_n should be included in the equation in determining the blunting corrected crack length a_{bi}. To achieve this, it is proposed in this paper that Eq. (2) be modified as follows

$$a_{bni} = a_0 + \frac{d_n J_i}{2\sigma_{YS}} \tag{7}$$

where a_{bni} is the strain hardening corrected blunting crack length and the second term is based on Eqs. (6a) and (6b). As Young's modulus (E) is almost constant for steels, d_n decreases with the decrease of strain hardening exponent and yield strength, as shown in Fig.2. From Eq. (7), the blunting corrected crack length a_{bi} increases with the decrease of d_n. Thus, it is more necessary to modify Eq. (2) with d_n for materials with smaller strain hardening exponent and yield strength.

With Eq. (7), Eq. (1) can be modified as follows

$$P_{Nni} = \frac{P_i}{WB\left(1 - \frac{a_{bni}}{W}\right)^{\eta_{pl}}} \tag{8}$$

where P_{Nni} is the strain hardening corrected i^{th} normalized load. Since the proposed correction is on blunting crack length as shown in Eq. (7), the modified normalization method is referred to as a blunting crack length corrected normalization method, denoted as CNM in this paper.

It should also be noted that according to ASTM E1820 A15 [2], the final crack extension of specimens is limited to 4 mm or $0.15(\mathrm{W} - a_0)$ when NM is used but this limit is usually not followed by researchers [13, 26, 27, 29, 32, 33]. There is difficulty in complying with this crack extension limit in some studies for a number of reasons [33]. For example, test results from Dzugan and Viehrig [26] indicated that exceeding the crack extension limit did not cause extensive errors for CT and SE(B) specimens by the normalization method. Test results from Gao et al. [38] concurred this argument. Thus, in this study, the crack extension limit was also

not followed in obtaining the full *J*-R curves, as did by many other researchers [5, 11, 14, 32, 33, 36-38, 44].

3. EXPERIMENT

To verify the performance of the developed CNM, a series of tests for different steels in a total of 12 specimens were carried out to obtain the *J*-R curves and fracture toughness. Since the strain hardening corrected blunting crack length a_{bni} largely depends on material properties, the grade of steel was selected as the test variable.

3.1 Test Specimen

Three types of commonly used Australian structural steel were tested for their fracture toughness: Weldox 700, G350 and G250. The same steels were also used in Gao et al. [33] for different purposes there. The strain hardening exponent and yield strength of these three types of steel cover a wide range. The mechanical properties of the specimens are taken from [33] as shown in Table 1. The true stress-strain curves can be seen in [33] and hence are not shown here. It should be noted that the strain hardening level is inversely proportional to the strain hardening exponent.

Table 1 Mechanical properties of test materials [33]

The specimens for three-point bending tests were cut from 16 mm and 10 mm thickness steel plates, with the dimensions of 160 mm × 32 mm × 16 mm and 100 mm × 20 mm × 10 mm. Six tests were carried out for each thickness of the specimen. These specimens were pre-cracked by fatigue loading according to ASTM E1820 [2], and then were side grooved to the thickness reduction of 20%. The initial crack lengths were all in the range of 0.45 to 0.7 W and the radius

of the side-grooved tip was around 0.65 mm following ASTM E1820. The configurations of three-point bending specimens are shown in Fig. 3.

Figure 3 Specimens for three-point bending tests (mm): (a) 16 mm thickness; (b) 10 mm thickness

3.2 Test Method

Table 2 shows the revised equations for calculating the strain hardening corrected blunting crack length a_{bni}, based on d_n in Fig. 2 [40, 42]. Two specimens were tested for each type of steel with a certain thickness and numbered as 01 and 02. All tests were carried out under quasi-static loading conditions under room temperature. The load-CMOD curves for the three-point bending G250 16 mm specimen 01 with unloading-reloading cycles are shown in Fig. 4 as an example. The load-CMOD curves of other specimens are similar and thus not repeated here. The data used for the normalization method are taken from the envelope curves of the unloading compliance experiments.

Table 2 d_n and a_{bni} for different materials

Figure 4 Load-CMOD records for three-point bending G250 16 mm specimen 01

After the tests, all specimens were heat tinted under 300℃ for 30 minutes. They were then refrigerated and broken in accordance with ASTM E1820 [2]. The final crack length of a specimen was measured with a digital imaging tool following the nine-point average method recommended in BS 7448-4 [3]. Fig. 5 shows the typical fracture surfaces of 16 mm and 10 mm SE(B) specimens for each type of steel. As can be seen, at the crack tips of these specimens, nearly straight lines are formed along the crack front for all specimens. When the straight lines are formed along the crack front, the tested fracture toughness is referred to as plane strain

fracture toughness [40]. Side-groove can eliminate the shear fracture part and provides an accurate measure of the resistance of the specimen to flat fracture, achieving the plane strain fracture toughness [40]. Fig. 5 confirms the plane strain conditions for crack growth in specimens. Therefore, Fig. 2(b) is used to determine d_n in this paper.

Figure 5 Typical fracture surfaces of specimens: (a) Weldox700, (b) G350, (c) G250. (major unit 10 mm)

3.3 Analysis of Test Results

The normalized load vs normalized plastic crack mouth opening displacement (CMOD) curves were obtained from the load-CMOD records. Figs. 6-7 show the typical curves obtained by NM and CNM for 16 mm specimen 01 of each steel. For other specimens of each steel, similar curves were also obtained and thus not repeated here. The final physical crack length was measured from the fracture surface and was used, together with the final load, to determine the anchor point. Subsequently, regression was performed to determine the coefficients *a, b, c*, and *d* of Eq. (A15.5) in ASTM E1820 A15 [2].

Figure 6 Normalized load vs normalized plastic CMOD curves for: (a) Weldox700 16 mm specimen 01; (b) G350 16 mm specimen 01

Figure 7 Normalized load vs normalized plastic CMOD curves for G250 16 mm specimen 01

With the determined *a, b, c*, and *d*, an iterative procedure was carried out to determine the crack length a_i for each load P_i. Then based on a_i, the *J*-integral and *J*-R curves were obtained by Eq. (1) and Eq. (8) respectively for the normalization method (NM) and the developed CNM. For Weldox700 and G350, the regression curves obtained by NM and CNM are nearly identical, as can be seen from Figs. 6(a) and 6(b), resulting in almost the same coefficients *a, b, c*, and *d.*

and hence identical *J*-R curves. Therefore, the modification for the blunting corrected crack length a_{bi} is not necessary for Weldox700 and G350 steels as NM is accurate for these materials. On the other hand, the regression curves obtained by NM and CNM are sharply different for G250 steel, as can be seen from Fig. 7, indicating the necessity to modify the blunting corrected crack length a_{bi} as proposed above.

The *J*-R curves obtained from the specimens by the unloading compliance method (UC) and normalization method (NM) are shown in Fig. 8-9, where 'UC 1' and 'NM 1' denote the *J*-R curve obtained for specimen 01 by UC and NM, respectively, while 'UC 2' and 'NM 2' are for specimen 02. The straight lines are 0.2 mm offset lines recommended by different standards for determining fracture toughness. The fracture toughness of the tested SE(B) specimens was obtained following ASTM E1820 [2], ISO 12135 [4] and BS 7448-4 [3], as presented in Table 3.

Table 3 Fracture toughness of Weldox700 and G350 steels

Figure 8 *J*-R curves of Weldox700 specimens using unloading compliance and normalization methods (a) 16 mm; (b) 10 mm

Figure 9 *J*-R curves of G350 16mm specimens using unloading compliance and normalization methods (a) 16 mm; (b) 10 mm

However, for G250, the regression curves obtained by NM and CNM are different, resulting in different coefficients *a, b, c*, and *d*, and hence different *J*-R curves for each method. Modification of blunting corrected crack length a_{bi} does affect the *J*-R curve of G250 steel. Fig. 10 presents the *J*-R curves obtained from two 16 mm specimens by UC, NM and CNM for two G250 specimens as denoted by 'UC', 'NM' and 'CNM'. The CNM is also applied to the G250 10 mm specimens to investigate its performance on different sizes of specimens with the same material. The obtained *J*-R curves are shown in Fig. 11. From Figs. 10-11 it can be seen that

352 the *J*-R curves determined by UC and CNM are almost identical when the crack extension is
353 smaller than 0.2 mm. Otherwise, the *J*-R curves determined by UC and NM are noticeably
354 different, especially for 16 mm thickness specimens. The *J*-R curve determined by CNM is
355 closer to that determined by UC than that by NM.

356 **Figure** 10 *J*-R curves of G250 16 mm specimen 01 and 02 using unloading compliance
357 method (UC), normalization method (NM) and corrected normalization method (CNM): (a)
358 G250 16 mm specimen 01; (b) G250 16 mm specimen 02

359 **Figure** 11 *J*-R curves of G250 10 mm specimen 01 and 02 using unloading compliance
360 method (UC), normalization method (NM) and corrected normalization method (CNM): (a)
361 G250 10 mm specimen 01; (b) G250 10 mm specimen 02

362

363 Since the method for fracture toughness recommended in ISO 12135 is the same as that in $J_{0.2BL}$
364 method in BS 7448-4, ISO 12135 is used for further discussion in this paper to avoid confusion
365 of these two methods. The deviation in fracture toughness as determined by UC, NM and CNM
366 in accordance with different standards is shown in Table 4. It can be found that the deviation
367 between UC and CNM is smaller than that between UC and NM for all G250 specimens and
368 by all standards. This effectively verifies that CNM can provide more accurate results than NM
369 for materials with small strain hardening exponent and yield strength, such as G250 steel.

370 It is also found from Table 3 and 4 that the difference in fracture toughness as determined by
371 UC and NM is smaller for steels with large strain hardening exponent and yield strength, such
372 as, Weldox700 steel, than for steels with small strain hardening exponent and yield strength,
373 such as, G250 steel. This again vindicates the need to modify the normalization method to allow
374 for the effect of mechanical properties, namely strain hardening exponent and yield strength,
375 on fracture toughness.

376 **Table** 4 Fracture toughness of G250 following different standards: (a) ASTM E1820; (b) ISO
377 12135; (c) BS 7448-4

3.4 Verification of CNM

It has been proved above that CNM performs better than NM, but it should be noted from Figs. 10-11 that difference in *J*-R curves between UC and CNM still exists after the blunting crack length is corrected. This difference is attributed to the intrinsic error in UC not in CNM. UC is used as benchmark because it is the best available method. More specifically, the difference is because of the considerable deformation of the specimens in the later stage of loading. This large deformation causes the thickening of the specimen (in the transverse direction) during the tests [38]. For example, it can be seen from Fig. 5(c) that the thickness of the remaining part of the specimen after the test is larger than its original thickness by about 20% because of the plastic swelling in the transverse direction. This will lead to an underestimation of the real thickness (B) of the specimen and, consequently, the over-estimation of the depth of the remaining part for the same value of compliance. As a result, the final crack length is underestimated by the UC method [38], which leads to a disagreement between UC and CNM. The underestimation of crack length by UC also can be theoretically explained as follows.

According to ASTM E1820-18 [2], the crack length can be determined by

$$a_i = [0.999748 - 3.9504u + 2.9821u^2 - 3.21408u^3 + 51.51564u^4 - 113.031u^5] \times W \qquad (9)$$

where W is the specimen width and u can be determined as follows

$$\mathrm{u} = \frac{1}{\left[\frac{4WEB_eC_i}{S}\right]^{0.5} + 1} \qquad (10)$$

in which C_i is the elastic compliance of the specimen and $\mathrm{C}_i = \left(\frac{\Delta V_i}{\Delta P_i}\right)$, V_i is the i^{th} CMOD, P_i is i^{th} load, $B_\mathrm{e} = B - \frac{(B-B_N)^2}{B}$ and B_N is the net thickness.

Once the crack lengths are determined, the corresponding *J*-integral can be calculated, and then the *J*-R curve can be obtained. The *J*-integral corresponding to the instantaneous crack length a_i can be calculated by following equations in ASTM E1820-18 [2].

For UC, the crack length at an arbitrary point (P_i, V_i) on the *P*-*V* curve is determined from Eqs. (9) and (10). After the specimen starts to thicken due to the crack extension, the stiffness of the specimen increases. This means that larger increment in load (ΔP_i) is required to produce the corresponding increment in CMOD (ΔV_i). Thus, at an arbitrary point on the *P*-*V* curve (P_i, V_i), the elastic compliance after thickening ($C_{i\mathrm{T}}$) is smaller than the non-thickening one (C_i). From Eqs. (9) and (10) it can be seen that the crack length after thickening ($a_{i\mathrm{T}}$) corresponding to this point (P_i, V_i) is smaller than the crack length without thickening (a_i), i.e., $a_{i\mathrm{T}} < a_i$. As a result, the crack length is underestimated in UC [38]. In other words, although the unloading-reloading *P*-*V* curves can be obtained accurately with the advanced digital program, the calculation procedures of UC cannot determine the crack length as accurately as the proposed CNM.

Moreover, the thickening is larger for materials with lower yield strength, for which the plastic deformation is more easily to occur, and the test results shown in [33, 38] suggest that thickening increases with the decrease of yield strength of the material. Therefore, the underestimation of crack length in UC increases with the decrease of yield strength of the material.

Also, the underestimation of crack length by UC increases with the crack extension. This underestimation leads to a more elevated *J*-R curve (higher in the vertical axis) for the UC method, especially for materials with small strain hardening exponent and yield strength. However, when the crack extension is small, the plastic deformation was small and such thickening did not occur. In other words, there should be no overestimation of thickness and hence no underestimation of crack length by the UC method when the crack extension is small.

Therefore, for the small crack extension, the *J*-R curves determined using UC and CNM nearly identical, which has been proved in Figs. 10-11.

As the underestimation of crack extension does not occur in cases of small crack extension, the crack extension corresponding to $J_{0.2}$ determined by the UC method is accurate. As a result, the underestimation of the final crack length does not affect the accuracy of $J_{0.2}$ determined by the UC method. Thus, the $J_{0.2}$ determined by UC is correct. As shown in Table 4(c), nearly identical $J_{0.2}$ (mean difference of 5.8% of the four tested specimens) is obtained by UC to that by the developed CNM, which again verifies the accuracy of the developed CNM. Moreover, it can also be seen from Figs.10-11 that the crack extensions at the early stage for both UC and CNM match very well because of the modification of blunting crack length, which further verifies the accuracy of the developed CNM.

When the crack extension increases, the underestimation of crack length by the unloading compliance (UC) method becomes increasingly prominent, and the *J*-R curve determined by UC becomes increasingly higher than the supposedly accurate *J*-R curve. Thus, the difference in $J_{0.2BL}$ and J_{Ic} as determined by UC and CNM exists because the corresponding crack extension is not small. For example, when the crack extensions of the 4 tested G250 steel specimens corresponding to J_{Ic} are all larger than 1.6 mm, which is much larger than 0.2 mm, the J_{Ic} determined by UC for G250 steel is overestimated. Therefore, the differences between $J_{0.2BL}$ and J_{Ic} determined by UC and CNM are caused by the underestimation of the crack extension by UC rather than due to the performance of the developed CNM.

For the comparison between NM and CNM, the crack length (a_i) is determined through an iterative procedure using the measured final crack length and a regression curve. The elastic compliance (C_{Ni}) used in NM and CNM for determining the crack length (a_i) is expressed as follows

$$C_{Ni} = \frac{6Sa_{bi}}{EW^2B_e} \times \left[0.76 - 2.28\left(\frac{a_{bi}}{W}\right) + 3.87\left(\frac{a_{bi}}{W}\right)^2 - 2.04\left(\frac{a_{bi}}{W}\right)^3 + \frac{0.66}{\left(1-\frac{a_{bi}}{W}\right)^2}\right] \quad (11)$$

where C_{Ni} is the specimen elastic compliance of CMOD at crack length a_{bi}, S is the span, a_{bi} is blunting corrected crack length and σ_Y is the effective yield strength. It can be seen from Eq. (11) that C_{Ni} is calculated based on a_{bi}. The calculation procedure in NM and CNM is almost not influenced by the specimen thickening. Therefore, the crack length determined using NM and CNM is almost not influenced by the large plastic deformation of the specimen. The infinity assumption of strain hardening exponent causes the NM not to performs well for small crack extensions, as explained above. However, such caused errors decrease with the crack extension and become not important for large crack extensions as shown in Figs. 10-11.

Thus, the developed CNM is verified theoretically and experimentally above. It can be established that the UC is correct for small crack extension and the NM is correct for the large crack extension. CNM agrees with UC for the small crack extension and with NM for the large crack extension. Therefore, the developed CNM is accurate for both large and small crack extensions and performs better than UC and NM.

4. DISCUSSION

4.1 Mechanical Properties of Materials

The accuracy of the developed CNM directly depends on the mechanical properties of materials, in particular, strain hardening exponent and yield strength. The effectiveness of blunting crack length correction is directly proportional to the difference between the blunting corrected crack length a_{bi} and the strain hardening corrected blunting crack length a_{bni}, i.e., Δa_{bni}. There is no agreed equation for determining a_{bi} in the normalization method (NM), and the most

commonly used equations of a_{bi} are Eq. (2) and (3). However, as it has been explained in Section 2 σ_{YS} should be used instead of σ_Y to calculate Δa_{bi}. It is thus reasonable to modify Eq. (2) of a_{bi} as follows

$$a_{bi} = a_0 + \frac{J_i}{2\sigma_{YS}} \tag{12}$$

It should be noted that Eq. (12) is the closest form of a_{bi} compared with a_{bni}. Thus, if the agreement in fracture toughness between UC and CNM is closer than that between UC and NM by using equation (12), the CNM will perform better than NM for all other forms of equations for a_{bi}.

From Eqs. (7) and (12), the overestimation of crack length (Δa_{bni}) because of the assumption of infinite *n* can be calculated as:

$$\Delta a_{bni} = a_{bi} - a_{bni} = \frac{J_i}{2}\left(\frac{1-d_n}{\sigma_{YS}}\right) \tag{13}$$

It can be seen that Δa_{bni} is influenced by J_i, σ_{YS} and d_n. The difference in *J*-R curves determined by NM and CNM is proportional to Δa_{bni}. Thus, the performance of the developed CNM is also proportional to the magnitude of Δa_{bni}. To ensure the magnitude of Δa_{bni} is large enough, either J_i or $\left(\frac{1-d_n}{\sigma_{YS}}\right)$ cannot be too small. For J_i, it is proportional to the area under the *P*-CMOD curve, A_i. The area A_i depends on the mechanical properties of the material and the geometry of the specimen. As both a_{bi} and a_{bni} are obtained from the same specimen, the influence of geometry can be ignored, which means A_i and J_i only depend on the mechanical

properties of the material. As A_i is a variable, it is reasonable to use the critical value of A_i corresponding to the fracture toughness to quantify the effect of J_i on Δa_{bni}.

Menezes et al. [32] indicated that $J_{0.2}$ method is the best one to determine initiation fracture toughness. Moreover, as J_{Ic} and $J_{0.2BL}$ are affected by the yield strength [33], $J_{0.2}$ is used to represent fracture toughness to avoid double counting of the yield strength on Δa_{bni}. Therefore, J_i can be represented by the fracture toughness ($J_{0.2}$), and the overestimation of the crack length corresponding to $J_{0.2}$ can be represented by the difference in crack length corresponding to $J_{0.2}$, i.e., $\Delta a_{0.2b}$. For d_n, it depends on n and σ_{YS} of the steel (E is almost the same), but the strain hardening exponent n plays a major role in determining d_n as shown in Fig. 2. The effect of σ_{YS} is relatively small. Therefore, the magnitude of $\Delta a_{0.2b}$ depends on the mechanical properties of the material only, such as $J_{0.2}$, n, and σ_{YS}, and the performance of CNM is influenced by $\Delta a_{0.2b}$.

The experimental results in Table 5 confirm that the performance of CNM depends on the difference in crack length corresponding to $J_{0.2}$, i.e., $\Delta a_{0.2b}$, which is $\Delta a_{0.2b} = \frac{J_{0.2}}{2}\left(\frac{1-d_n}{\sigma_{YS}}\right)$ as listed in Table 5 for the tested materials. For Weldox700, the strain hardening exponent is large (9.94), resulting in a relatively large value of d_n (0.59). Although the fracture toughness ($J_{0.2}$) is not small (301 kJ/m^2), a small value of $\Delta a_{0.2b}$ (0.08 mm) is obtained, due to a large yield strength (774MPa). For G350, the fracture toughness ($J_{0.2}$) is small (146 kJ/m^2). Although the strain hardening exponent and yield strength are not large (5.76 and 438 MPa, respectively), the value of $\Delta a_{0.2b}$ is also small (0.075 mm). When $\Delta a_{0.2b}$ is small, the regression curves corrected by the blunting crack length are nearly identical with the non-corrected ones, according to Fig. 8-9, which means the correction for these materials is not necessary, and the

normalization method performs well for these materials. Table 3 shows that the deviation in $J_{0.2}$ (column 4) between using UC and NM is small (less than 10%). Therefore, the blunting crack length correction for a_{bi} is not necessary for materials with small value of $\Delta a_{0.2b}$, such as Weldox700 and G350.

Table 5 Values of $\Delta a_{0.2b}$

For G250, it has a relatively small strain hardening exponent (4.7), a low yield strength (302 MPa), and a large fracture toughness ($J_{0.2}$ = 423 kJ/m^2), resulting in a relatively large value of $\Delta a_{0.2b}$ (0.41 mm). From Figs. 10-11, it can be seen that the difference between the *J*-R curves as determined by UC and CNM is smaller than that determined by UC and NM when the crack extension is smaller than 0.2 mm, which is critical for determining fracture toughness ($J_{0.2}$). As illustrated in Table 4, the deviation in fracture toughness as determined by UC and CNM for both sizes of specimens is smaller than that determined by UC and NM following all standards. It is clear that the developed CNM increases the accuracy of fracture toughness for tested materials with a large value of $\Delta a_{0.2b}$.

4.2 Other Factors

Other factors that affect the accuracy of the developed CNM include the specimen thickness, ratio of initial crack length to width of the specimen (a_0/W) and the construction line used to determine the fracture toughness. Specimens with different thickness (10 mm and 16 mm) and a_0/W (from 0.51 to 0.67) were used in the tests. It can be seen from Table 4 that the agreement between UC and CNM is closer than that between UC and NM for all G250 specimens, regardless of the difference in thickness and a_0/W. It can also be seen from Table 4 that, when the average a_0/W of G250 10 mm specimens is almost equal to that of 16 mm specimens, the deviation between UC and NM or UC and CNM increases with the specimen thickness. This is

because of the more prominent plastic deformation for thicker specimens. The agreement between UC and CNM also increases with the increase of a_0/W for 16 mm specimens, but this trend cannot be found for 10 mm specimens. Therefore, the performance of CNM is influenced by the thickness of the specimens. It appears that more experiments are necessary to investigate the effect of a_0/W further.

From Tables 3 and 4, it can be seen that different values of fracture toughness are determined for the same material with different construction lines prescribed in standards. The slope of construction lines used to determine fracture toughness is $2\sigma_Y$, $3.75\sigma_{TS}$ and infinite for ASTM E1820, ISO 12135 and BS 7448-4 $J_{0.2}$ method, respectively. All these lines are not related to the strain hardening property of the material. The crack extension corresponding to the fracture toughness increases with the decrease of the construction line slope. Therefore, the difference in fracture toughness determined by UC and CNM is the smallest following BS 7448-4 $J_{0.2}$ method, while the largest difference is from ASEM E1820. According to Table 4(c), for CNM, the tested fracture toughness is nearly the same as that determined using UC if $J_{0.2}$ method is used following BS 7448-4, meaning that the performance of CNM is much better than that of NM. If the slope of the construction line is $3.75\sigma_{TS}$ as per ISO 12135, the performance of CNM is still much better than that of NM for all G250 specimens, as shown in Table 4(b). When the slope of the construction line is $2\sigma_Y$, the difference in the tested fracture toughness between using UC and CNM is the largest, as shown in Table 4(a). This is because the crack extension is underestimated by the UC method, as explained above. Therefore, the developed CNM performs better than NM following all standards, with the BS 7448-4 $J_{0.2}$ method the best.

5. CONCLUSIONS

In this paper, the normalization method has been analytically modified by incorporating the strain hardening in calculating the blunting corrected crack length. Experiments have been

undertaken to prove the underperformance of the normalization method for steels with small strain hardening and yield strength and to verify the modified normalization method (CNM). A comparison of fracture toughness determined by CNM with that by the unloading compliance method (UC) and the normalization method (NM) also corroborates the improved accuracy of the developed CNM. It has been found in the paper that the difference in J-integral as determined by the UC method and the developed CNM increases with the increase of crack extension and that the increasing underestimation of crack extension by UC is the main cause for the deviation in fracture toughness $J_{0.2BL}$ and J_{Ic} as determined by UC and CNM. It has also been found that the developed CNM performs very well for materials with small strain hardening exponent and yield strength and performs better for specimens with smaller thickness and in accordance with all standards. Whilst it is acknowledged that more experiments are useful to further verify the accuracy of the developed CNM, it can be concluded that the developed CNM has overcome the deficiency of the normalization method for steels with small strain hardening exponent and yield strength.

ACKNOWLEDGMENT

Financial support from the Australian Research Council under DP140101547, LP150100413 and DP170102211, and the National Natural Science Foundation of China with Grant No. 51820105014 is gratefully acknowledged.

REFERENCES

[1] G. Clarke, W. Andrews, P. Paris, D. Schmidt, Single specimen tests for J_{Ic} determination, in: Mechanics of Crack Growth, West Conshohocken, PA; ed. J. Rice and P. Paris, ASTM STP 590; 1976, p.27-42.

[2] ASTM E1820-18, Standard test method for measurement of fracture toughness, American Society for Testing and Materials, 2018.

[3] B.S. 7448-4:1997, Fracture mechanics toughness tests - part 4: method for determination of fracture resistance curves and initiation values for stable crack extension in metallic materials, British Standards Institution, 1997.

[4] ISO 12135:2016(E), Metallic Materials-Unified Method of Test for the Determination of Quasistatic Fracture Toughness, International Organization for Standardization, 2016.

[5] R. Herrera, J. Landes, A direct *J-R* curve analysis of fracture toughness tests, Journal of Testing and Evaluation 16(5) (1988) 427-449.

[6] J. Joyce, H. Ernst, and P. Paris. Direct Evaluation of J-Resistance Curves from Load Displacement Records. In: Fracture mechanics: twelfth conference, West Conshohocken, PA; ed. P. Paris, ASTM STP700; 1980, p.222-236.

[7] H. Ernst, P. Oaris, M. Rossow, J. Hutchinson, Analysis of load-displacement relationship to determine JR curve and tearing instability material properties, In: Fracture Mechanics: Proceedings of the Eleventh National Symposium on Fracture Mechanics, West Conshohocken, PA; ed. C. Smith, ASTM STP 677; 1979, p581-599.

[8] H. Ernst, Techniques of analysis of load-displacement records by *J*-integral methods, NUREG/CR-1222, Nyclear Regulatory Commission; 1980.

[9] H. Ernst, P. Paris, J. Landes, Estimations on J-integral and tearing modulus *T* from a single specimen test record. In:Fracture mechanics: thirteenth conference, West Conshohocken, PA; ed. R. Roberts, ASTM STP 743; 1981, p.476-502.

[10] M. Sharobeam, J. Landes, The load separation criterion and methodology in ductile fracture mechanics, International Journal of Fracture 47(2) (1991) 81-104.

[11] R. Herrera, J. Landes. Direct *J-R* curve analysis: a guide to the methodology. In: Fracture mechanics: twenty-first symposium, West Conshohocken, PA; ed. J. Gudas, J. Joyce, and E. Hackett, ASTM STP 1074; 1990, p.24-43.

[12] T.W. Orange. Method and models for R-Curve instability calculations. In: Fracture mechanics: twenty-first symposium, West Conshohocken, PA; ed. J. Gudas, J. Joyce, and E. Hackett, ASTM STP 1074; 1990, p.545-559.

[13] Z. Zhou, K. Lee, R. Herrera, J.D. Landes, Normalization: an experimental method for developing *J-R* curves, Elastic-plastic fracture test methods: the user's experience (second volume), West Conshohocken, PA; ed. J. Joyce, ASTM STP 1114; 1991, p.42-56.

[14] J. Landes, Z. Zhou, K. Lee, R. Herrera, Normalization method for developing *J-R* curves with the LMN function, Journal of Testing and Evaluation 19(4) (1991) 305-311.

[15] M. Scibetta, E. Lucon, J. Schuurmans, E. van Walle, Numerical simulations to support the normalization data reduction technique, Engineering Fracture Mechanics 73(4) (2006) 524-534.

[16] K. Lee, J.D. Landes, Developing *J-R* Curves Without Displacement Measurement Using Normalization, Fracture mechanics: twenty-third symposium, West Conshohocken, PA; ed. R. Chona, ASTM ATP1189; 1993, p.133-167.

627 [17] J.A. Joyce, Analysis of a high rate round robin based on proposed annexes to ASTM E
628 1820, Journal of Testing and Evaluation 29(4) (2001) 329-351.
629
630 [18] C. Bao, L. Cai, G. He, C. Dan, Normalization method for evaluating J-resistance curves of
631 small-sized CIET specimen and crack front constraints, International Journal of Solids and
632 Structures 94 (2016) 60-75.
633
634 [19] A. Cassanelli, H. Ortiz, J. Wainstein. Separability property and load normalization in AA
635 6061-T6 aluminum alloy. In: Fatigue and fracture mechanics: 32nd volume, West
636 Conshohocken, PA; ed. R. Chona, ASTM STP 1406; 2002, p.49-72.
637
638 [20] J. Landes, Z. Zhou, Application of load separation and normalization methods for
639 polycarbonate materials, International Journal of Fracture 63(4) (1993) 383-393.
640
641 [21] C. Morhain, J. Velasco, Determination of *J-R* curve of polypropylene copolymers using
642 the normalization method, Journal of Materials Science 36(6) (2001) 1487-1499.
643
644 [22] F. Baldi, T. Riccò, High-rate J-testing of toughened polyamide 6/6: Applicability of the
645 load separation criterion and the normalization method, Engineering Fracture Mechanics 72(14)
646 (2005) 2218-2231.
647
648 [23] R. Varadarajan, E. Dapp, C. Rimnac, Static fracture resistance of ultra high molecular
649 weight polyethylene using the single specimen normalization method, Polymer Testing 27(2)
650 (2008) 260-268.
651
652 [24] P.M. Frontini, L.A. Fasce, F. Rueda, Non linear fracture mechanics of polymers: Load
653 Separation and Normalization methods, Engineering Fracture Mechanics 79 (2012) 389-414.
654
655 [25] J. Dubey, S. Wadekar, R. Singh, T. Sinha, J. Chakravartty, Assessment of hydrogen
656 embrittlement of Zircaloy-2 pressure tubes using unloading compliance and load normalization
657 techniques for determining J–R curves, Journal of Nuclear materials 264(1-2) (1999) 20-28.
658
659 [26] J. Džugan, H.-W. Viehrig, Application of the normalization method for the determination
660 of *J–R* curves, Materials Science and Engineering: A 387 (2004) 307-311.
661
662 [27] X.-K. Zhu, J.A. Joyce, J–resistance curve testing of HY80 steel using SE (B) specimens
663 and normalization method, Engineering Fracture Mechanics 74(14) (2007) 2263-2281.
664
665 [28] X.-K. Zhu, B.N. Leis, Fracture resistance curve testing of X80 pipeline steel using the
666 SENB specimen and normalization method, Journal of Pipeline Engineering 7(2) (2008).
667
668 [29] X. Zhu, P. Lam, Y. Chao, Application of normalization method to fracture resistance
669 testing for storage tank A285 carbon steel, International Journal of Pressure Vessels and Piping
670 86(10) (2009) 669-676.
671
672 [30] C. Bao, L. Cai, K. Shi, C. Dan, Y. Yao, Improved normalization method for ductile fracture
673 toughness determination based on dimensionless load separation principle, Acta Mechanica
674 Solida Sinica 28(2) (2015) 168-181.
675

[31] G. He, C. Bao, L. Cai, Y. Wu, X. Zhao, Estimation of J-resistance curves of SA-508 steel from small sized specimens with the correction of crack tip constraint, Engineering Fracture Mechanics (2018).

[32] J.T.O. de Menezes, J.E.P. Ipiña, E.M. Castrodeza, Normalization method for JR curve determination using SENT specimens, Engineering Fracture Mechanics 199 (2018) 658-671.

[33] H. Gao, Y. Wu, C.-Q. Li, Performance of normalization method for steel with different strain hardening levels and effective yield strengths, Engineering Fracture Mechanics 218 (2019).

[34] X. Zhu, B. Leis, J.A. Joyce, Experimental estimation of *J*-R curves from load-CMOD record for SE (B) specimens. Journal of ASTM International 5(5) (2008) 1-15.

[35] E. Lucon, M. Scibetta, E. Valle, Applying the Normalization Technique for Measuring the Upper Shelf Toughness Properties of RPV Steels, Final report of Steel & Fusion project BLG-915, SCK•CEN, Mol, Belgium, 2002.

[36] C. Fortes, F. Bastian, A modified normalization method for developing *J*-R and CTOD-R curves with the LMN function, Journal of testing and evaluation 25(3) (1997) 302-307.

[37] Z. Liu, X. Wang, S. Shi, Y. Shen, X. Chen, Application of modified normalization method for JR curve determination using clamped SENT specimens with varying in-plane and out-of-plane constraints, Engineering fracture mechanics 230 (2020).

[38] H. Gao, C.-Q. Li, W. Wang, Y. Wang, B. Zhang, Factors affecting the agreement between unloading compliance method and normalization method, Engineering Fracture Mechanics (Accepted in June 2020).

[39] J. Landes, and J. Begley, Test results from J-integral studies: an attempt to establish a J_{Ic} testing procedure. In: Fracture analysis: proceedings of the 1973 national symposium on fracture mechanics, Part II, West Conshohocken, PA; ed. G. Irwin, ASTM STP560; 1974, p.170-186.

[40] T.L. Anderson, Fracture mechanics: fundamentals and applications, CRC press, 2017.

[41] J. Landes, The blunting line in elastic-plastic fracture, Fatigue & Fracture of Engineering Materials & Structures 18 (1995) 1289-97.

[42] C.Shih, Relationships between the *J*-integral and the crack opening displacement for stationary and extending cracks, Journal of the Mechanics and Physics of Solids. 29 (1981) 305-26.

[43] W. Ramberg, and W.R. Osgood, Description of stress-strain curves by three parameters, Technical Note No. 902, National Advisory Committee For Aeronautics, Washington DC, 1943.

List of Tables

733

734

735 Table 1 Mechanical properties of test materials

Material	E (GPa)	σ_{YS} (MPa)	σ_{TS} (MPa)	σ_{Y} (MPa)	n	α
Weldox 700	198	774	849	812	9.94	1.48
G350	203	438	522	480	5.76	10.8
G250	209	301	454	378	4.70	8.27

736

737

738

739

740

741

742

743

744

745

746

747

748

749

750

Table 2 d_n and a_{bni} for different materials

Material	σ_0/E	$1/n$	$\alpha^{1/n}$	d_n (plane strain)	a_{bi}
Weldox 700	0.0039	0.08	1.03	0.59	$a_{bni} = a_0 + 0.59\left(\frac{J_i}{2\sigma_{YS}}\right)$
G350	0.0022	0.17	1.51	0.55	$a_{bni} = a_0 + 0.55\left(\frac{J_i}{2\sigma_{YS}}\right)$
G250	0.0015	0.21	1.56	0.42	$a_{bni} = a_0 + 0.42\left(\frac{J_i}{2\sigma_{YS}}\right)$

Table 3 Fracture toughness of Weldox700 and G350 steels

Specimen	ASTM E1820-18 (J_{Ic}; kJ/m^2)				ISO 12135:2016 (E) ($J_{0.2BL}$; kJ/m^2)				BS 7448-4:1997 ($J_{0.2}$; kJ/m^2)			
	UC	NM	Deviation (%)		UC	NM	Deviation (%)		UC	NM	Deviation (%)	
16mm W700 01	699	604	13.59	15.47	585	524	10.43	8.05	272	246	9.56	6.84
16mm W700 02	605	500	17.36		459	433	5.66		291	279	4.12	
10mm W700 01	642	567	11.68	8.93	551	506	8.17	7.97	351	333	5.13	6.18
10mm W700 02	566	531	6.18		515	475	7.77		318	295	7.23	
16mm G350 01	223	186	16.59	20.96	183	166	9.29	15.00	143	138	3.50	10.14
16mm G350 02	225	168	25.33		198	157	20.71		149	124	16.78	
10mm G350 01	216	169	21.76	19.02	181	155	14.36	14.25	146	132	9.59	9.86
10mm G350 02	215	180	16.28		184	158	14.13		148	133	10.14	

Table 4 Fracture toughness of G250 following different standards:

(a) ASTM E1820

Specimen	a_0/W	ASTM E1820-18 (J_{Ic}; kJ/m^2)							
		UC	NM	Deviation (%)		UC	CNM	Deviation (%)	
16mm G250 01	0.67	1138	886	22.14	29.91	1138	941	17.31	24.16
16mm G250 02	0.51	1680	1047	37.68		1680	1159	31.01	
10mm G250 01	0.56	1219	903	25.92	25.74	1219	960	21.25	16.14
10mm G250 02	0.61	1233	918	25.55		1233	1097	11.03	

(b) ISO 12135

Specimen	a_0/W	ISO 12135:2016 (E) ($J_{0.2BL}$; kJ/m^2)							
		UC	NM	Deviation (%)		UC	CNM	Deviation (%)	
16mm G250 01	0.67	854	559	34.54	35.58	854	681	20.26	22.67
16mm G250 02	0.51	897	579	35.45		897	672	25.08	
10mm G250 01	0.56	810	639	21.11	16.64	810	735	9.26	6.96
10mm G250 02	0.61	814	715	12.16		814	776	4.67	

(c) BS 7448-4

Specimen	a_0/W	BS 7448-4:1997 ($J_{0.2}$; kJ/m^2)							
		UC	NM	Deviation (%)		UC	CNM	Deviation (%)	
16mm G250 01	0.67	489	331	32.31	32.82	489	456	6.75	7.20
16mm G250 02	0.51	366	244	33.33		366	394	7.65	
10mm G250 01	0.56	407	344	15.48	16.18	407	399	1.97	4.41
10mm G250 02	0.61	379	315	16.89		379	353	6.86	

819

820

821

822 Table 5 Values of $\Delta a_{0.2b}$

Material	Average $J_{0.2}$ (UC, kJ/m^2)	d_n	σ_{YS} (MPa)	$\Delta a_{0.2b}=J_{0.2}(1-d_n)/(2\sigma_{YS})$ (mm)
Weldox 700	301	0.59	774	0.08
G350	146	0.55	438	0.075
G250	423	0.42	301	0.41

823

824

825

826

827 **List of Figures**

847

848

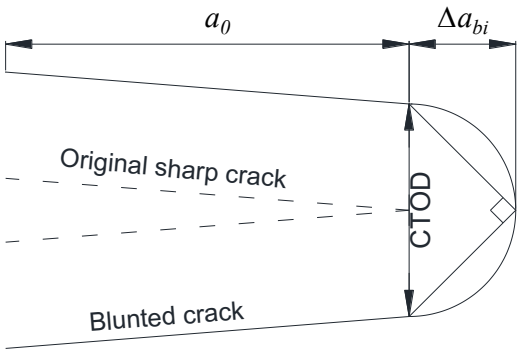

849

850 Figure 1 Blunted crack length ($a_{bi} = a_0 + \Delta a_{bi}$) [40]

851
852
853
854
855
856
857
858

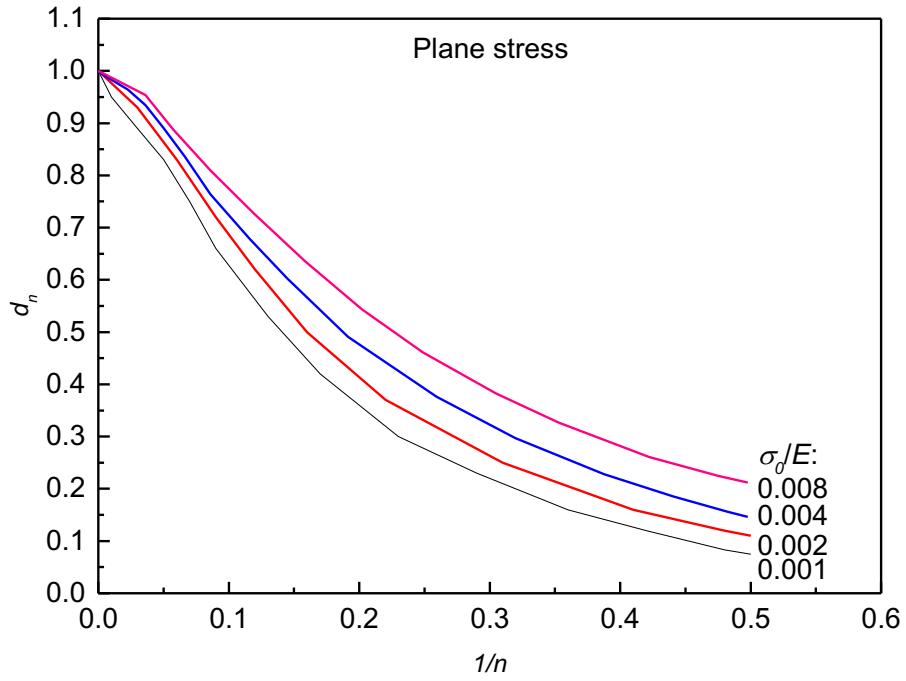

(a)

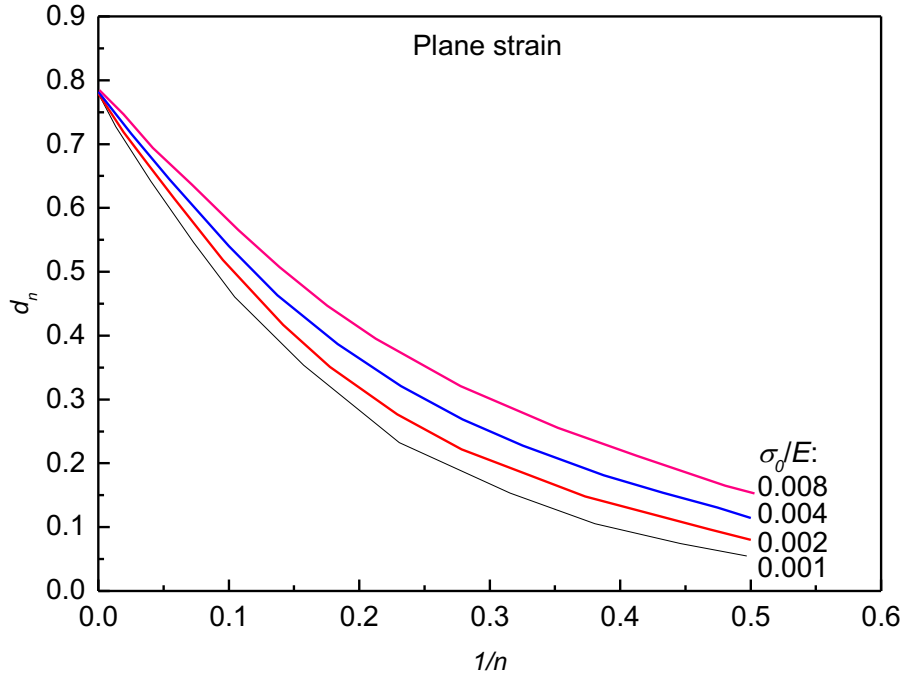

(b)

Figure 2 Value of d_n for plane stress (a) and plane strain (b) conditions with α=1

867

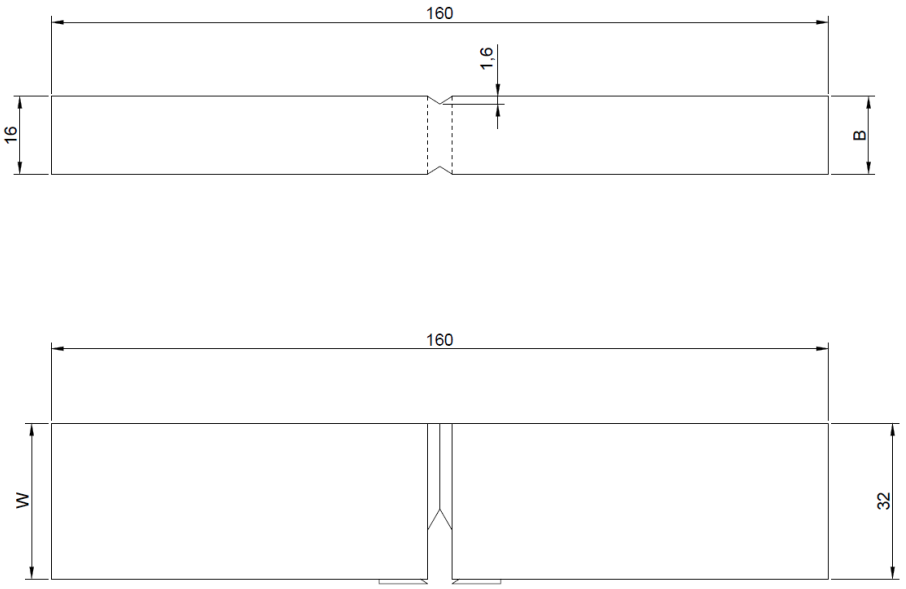

868

869 (a)

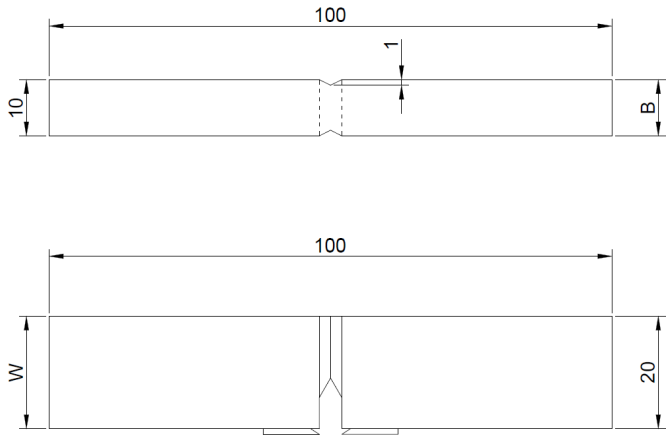

870

871 (b)

872 Figure 3 Specimens for three-point bending test (mm): (a) 16 mm thickness; (b) 10 mm
873 thickness

874

875

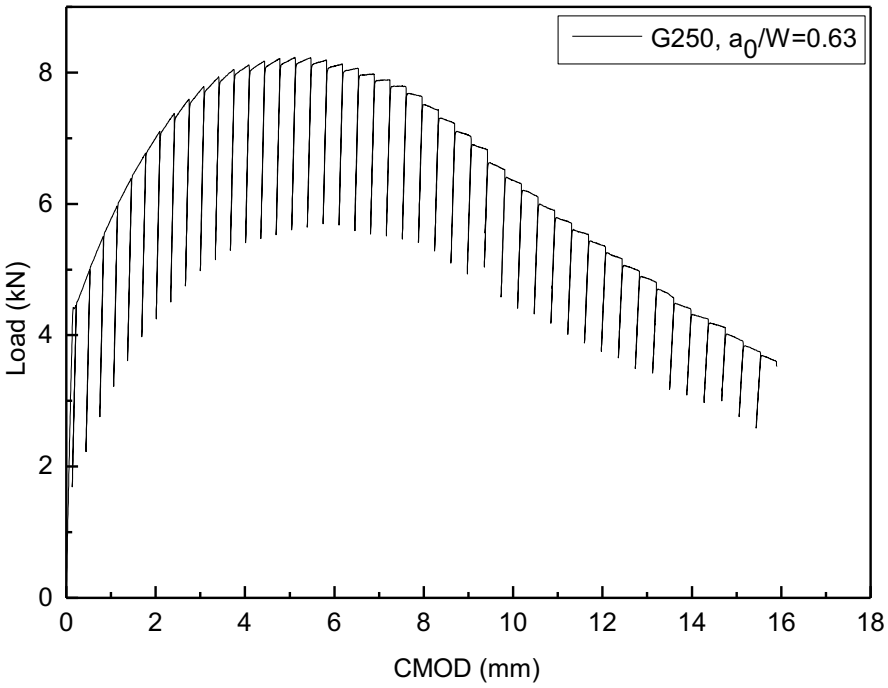

Figure 4 Load-CMOD records for there-point bending G250 16 mm specimen 01

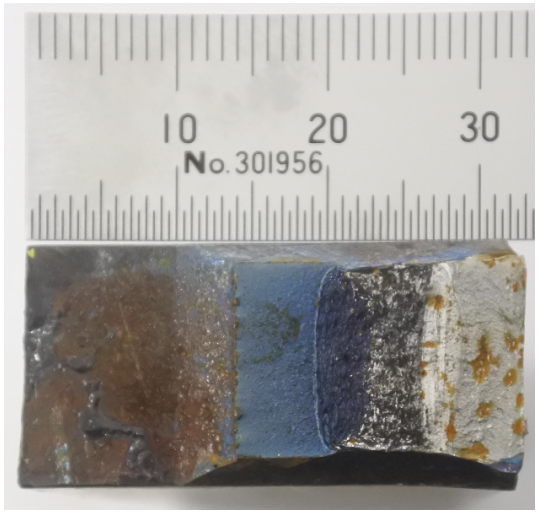

(a1 16 mm)

(a2 10 mm)

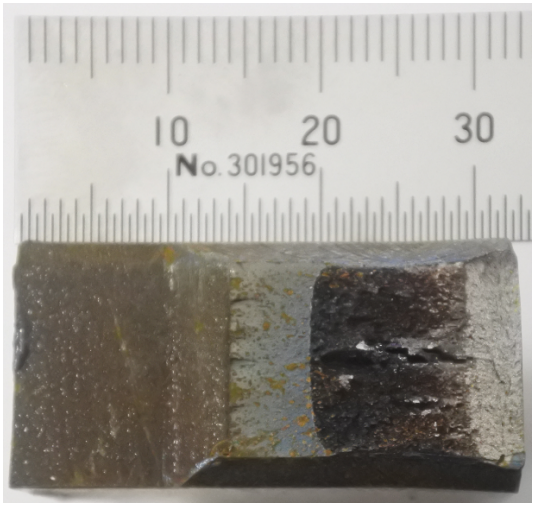

(b1 16 mm)

(b2 10 mm)

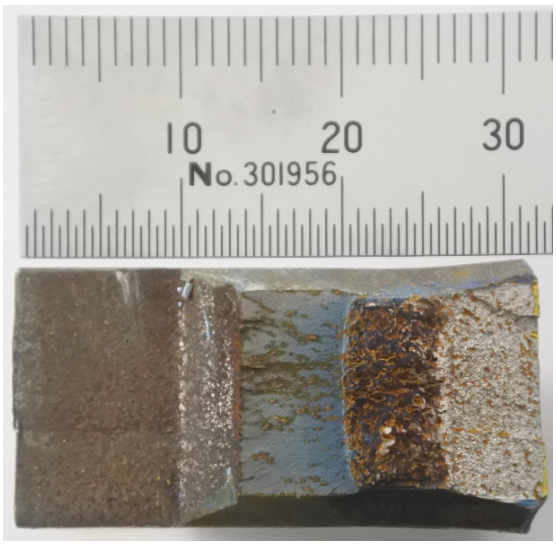

(c1 16 mm)

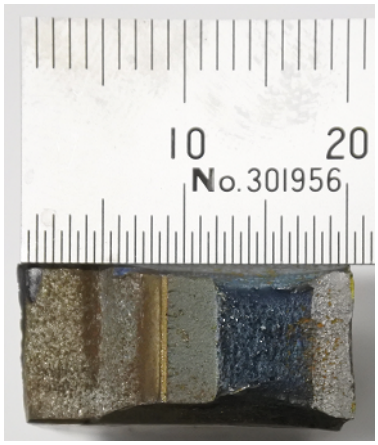

(c2 10 mm)

Figure 5 Typical fracture surfaces of specimens: (a) Weldox700, (b) G350, (c) G250. (major unit 10 mm)

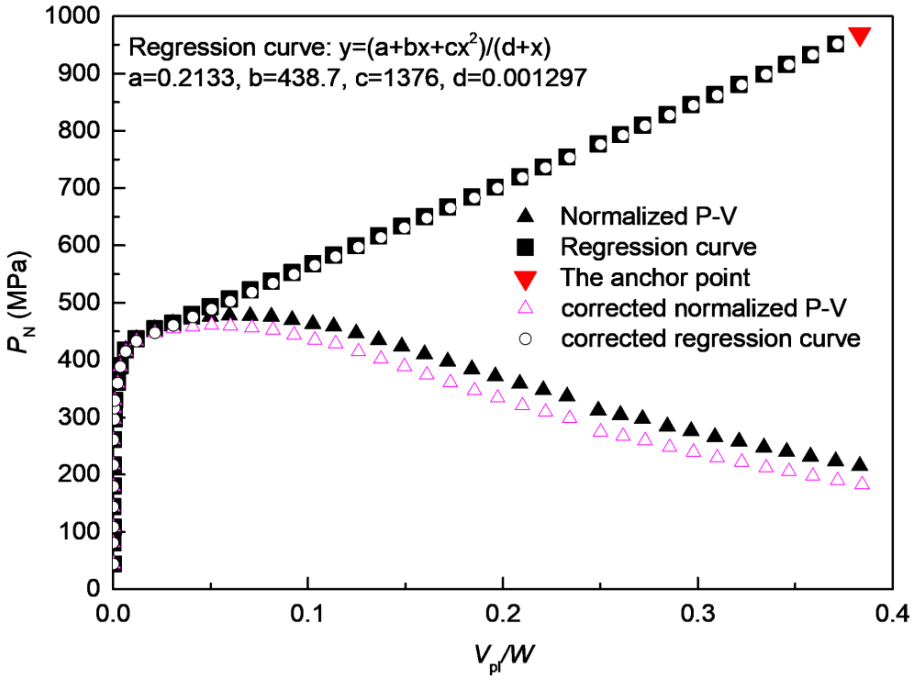

(a)

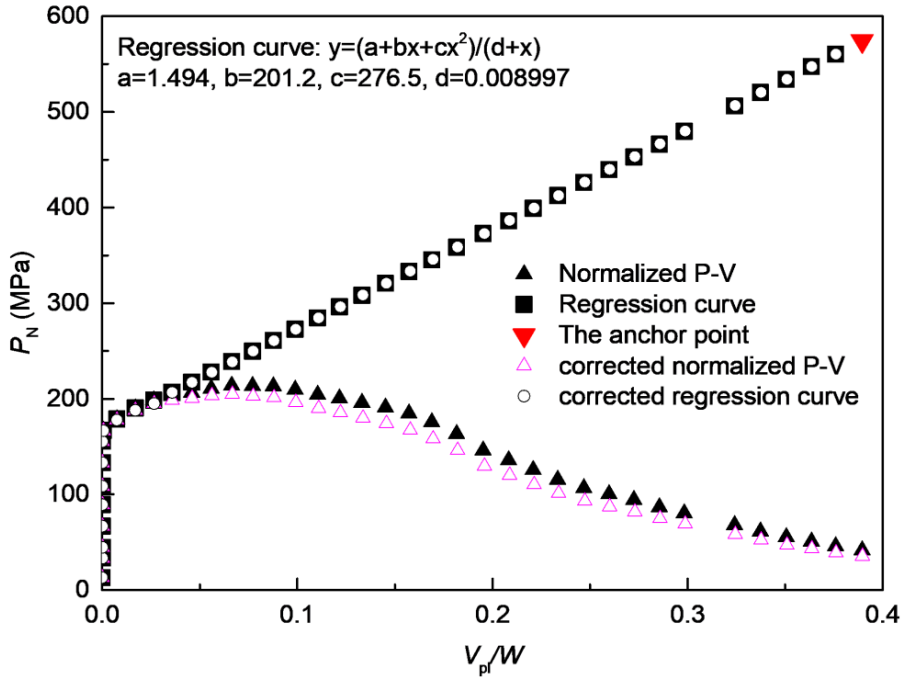

(b)

Figure 6 Normalized load vs normalized plastic CMOD curves for: (a) Weldox700 16 mm specimen 01; (b) G350 16 mm specimen 01

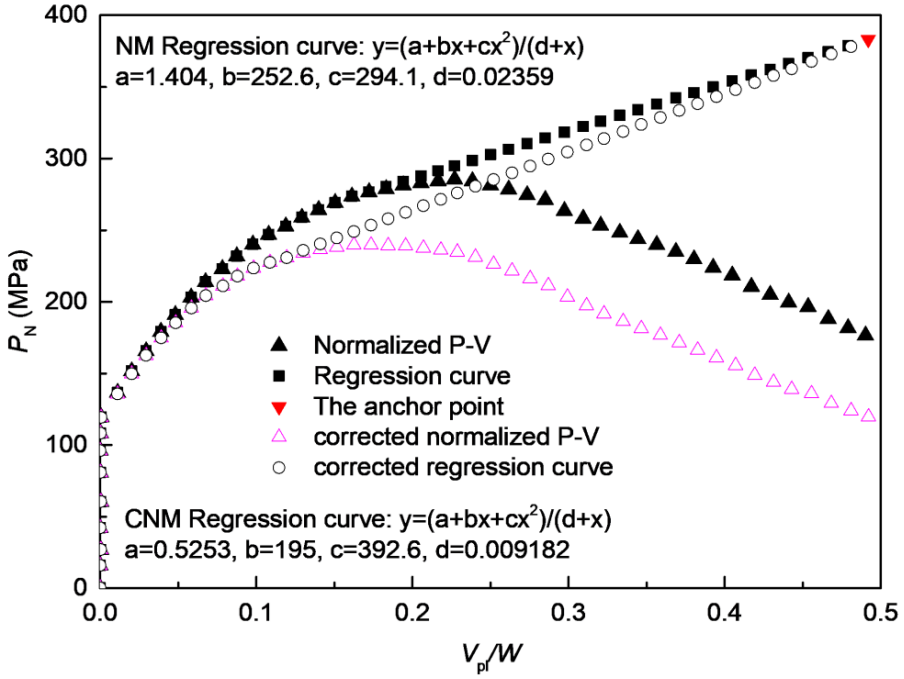

Figure 7 Normalized load vs normalized plastic CMOD curves for G250 16 mm specimen 01

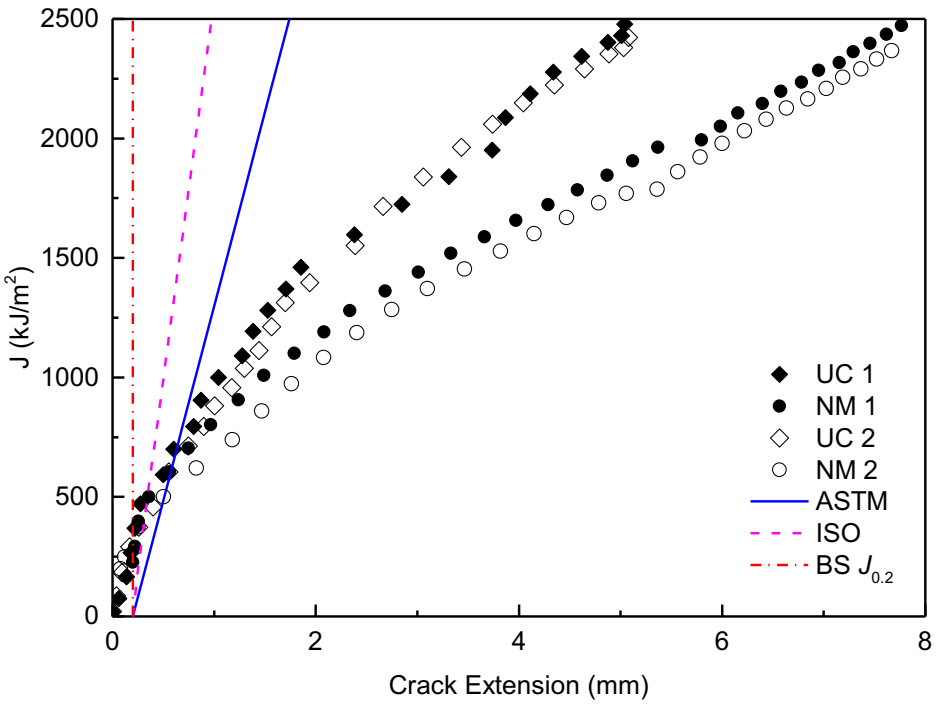

(a)

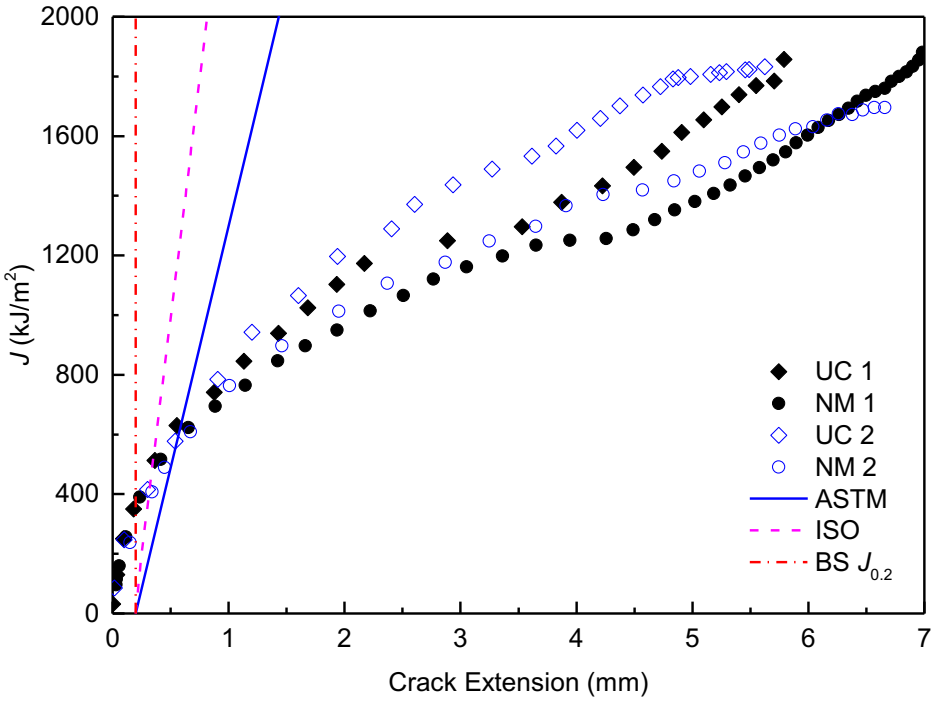

(b)

Figure 8 *J*-R curves of Weldox700 16 mm specimens using unloading compliance and normalization methods (a) 16 mm; (b) 10 mm

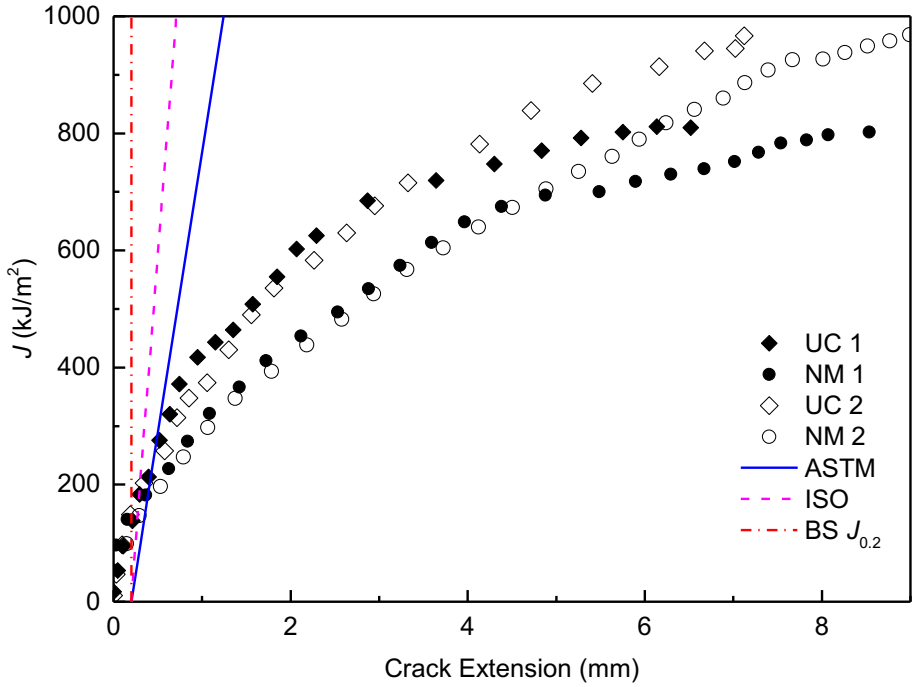

(a)

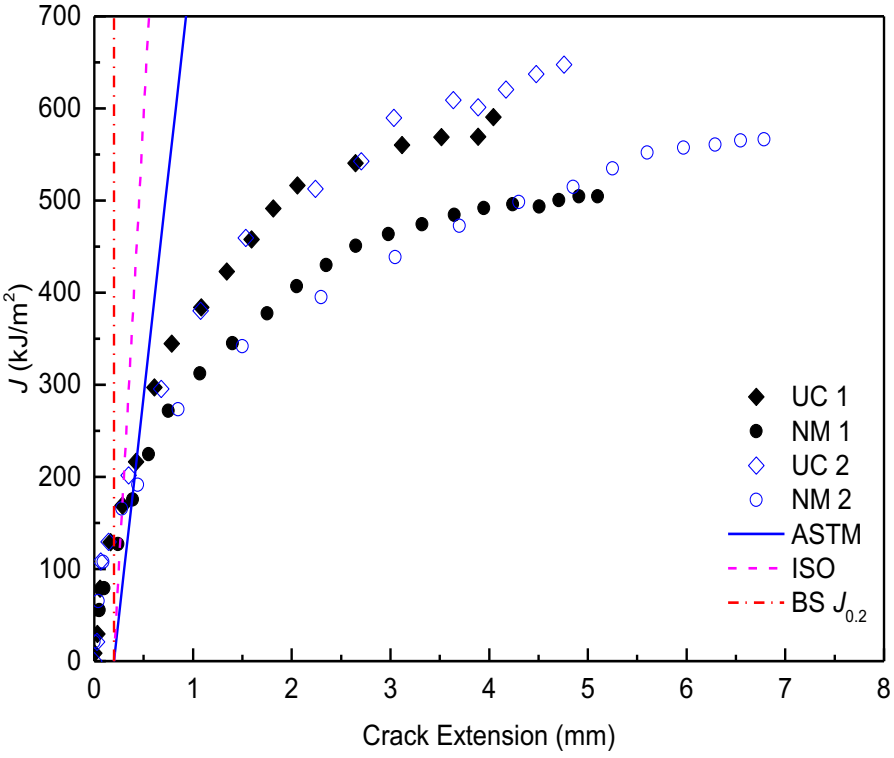

(b)

Figure 9 *J*-R curves of G350 16mm specimens using unloading compliance and normalization methods (a) 16 mm; (b) 10 mm

928

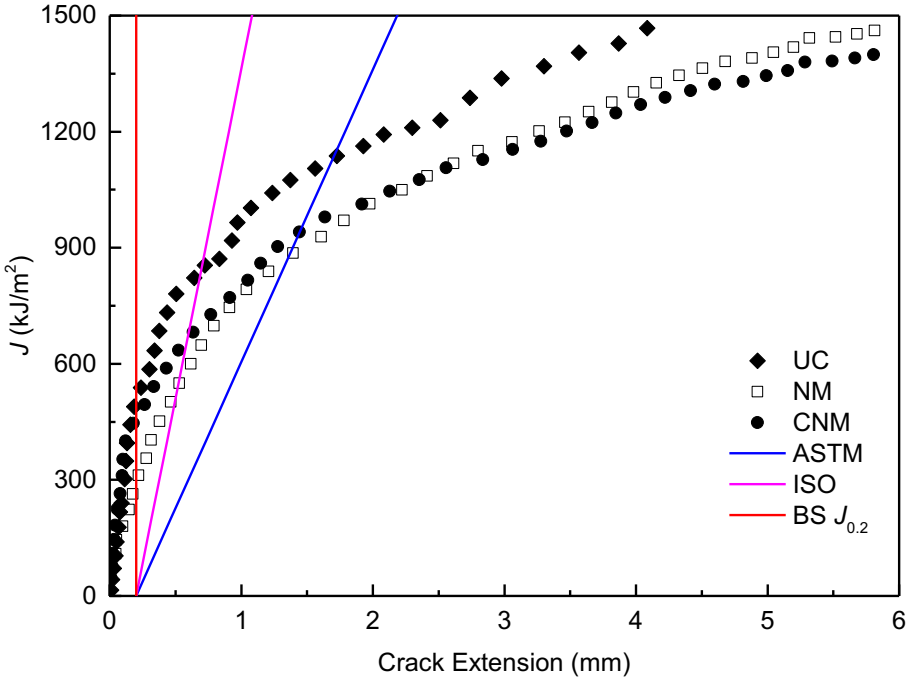

929

930 (a)

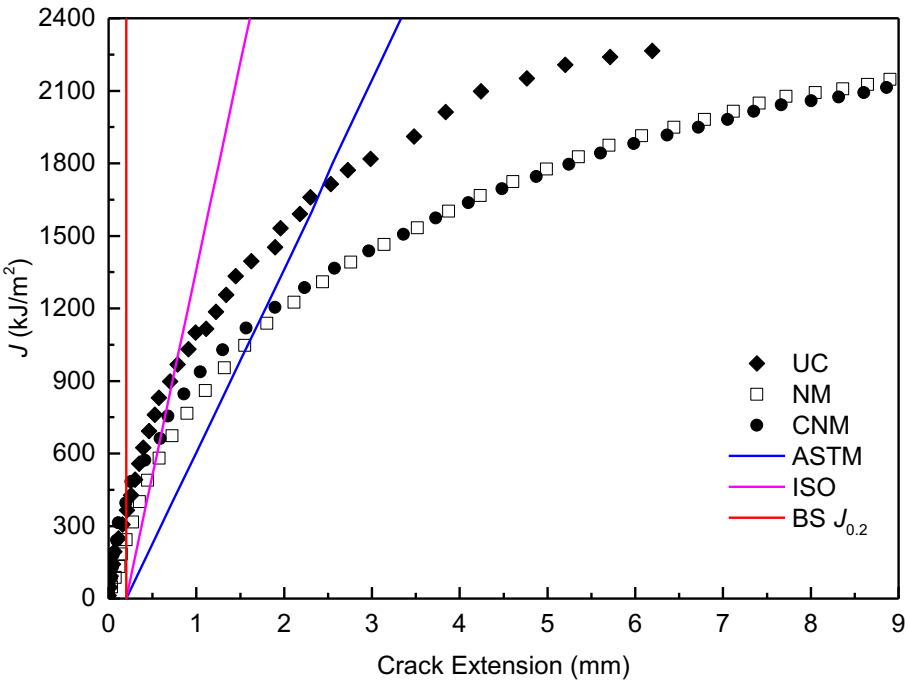

931

932 (b)

933 Figure 10 *J*-R curves of G250 16 mm specimen 01 and 02 using unloading compliance
934 method (UC), normalization method (NM) and corrected normalization method (CNM): (a)
935 G250 16 mm specimen 01; (b) G250 16 mm specimen 02

936

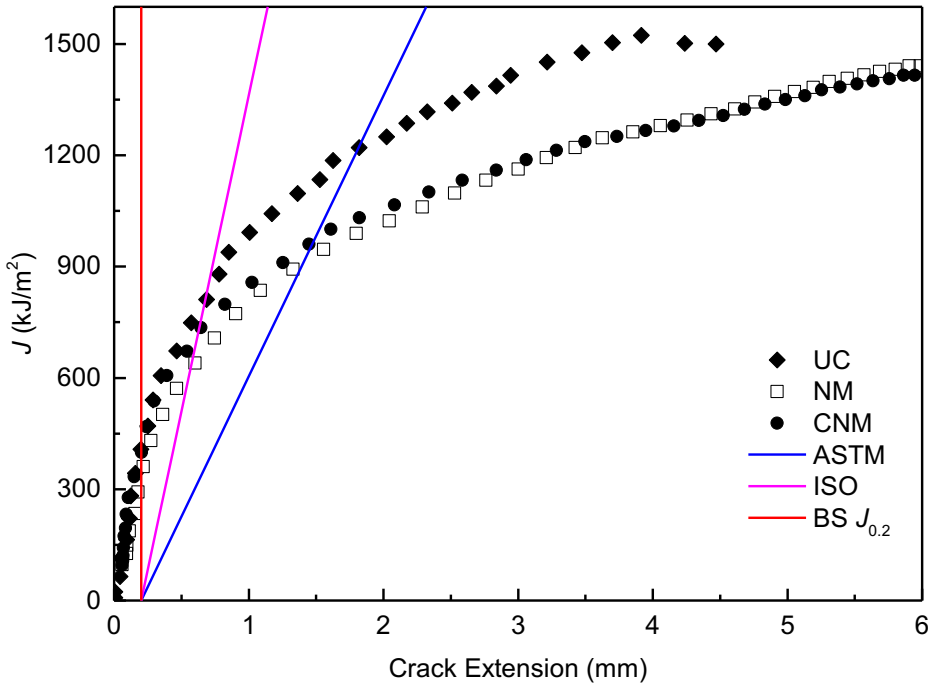

(a)

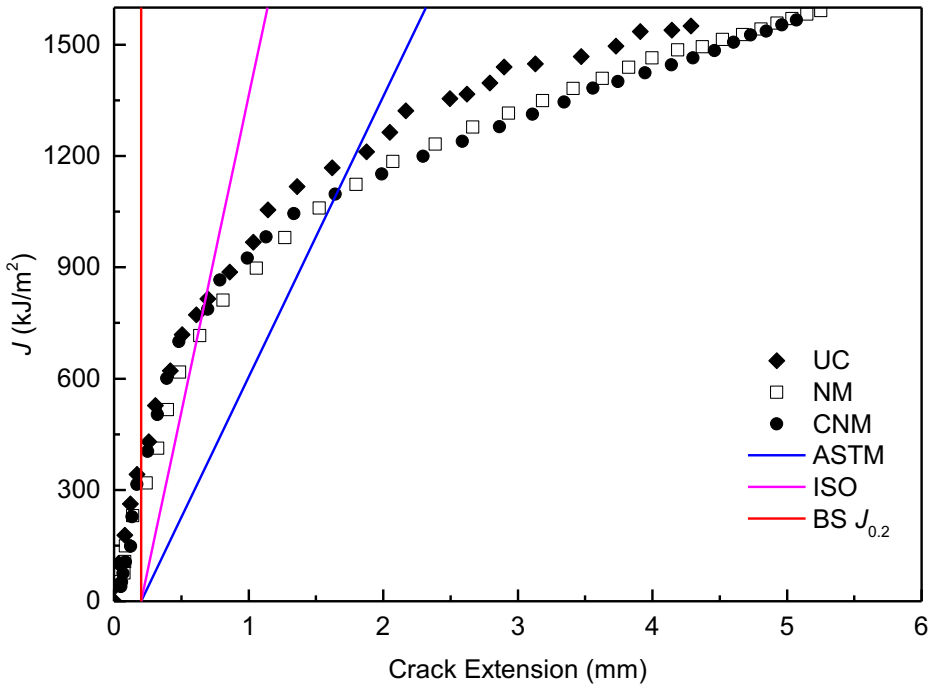

(b)

Figure 11 *J*-R curves of G250 10 mm specimen 01 and 02 using unloading compliance method (UC), normalization method (NM) and corrected normalization method (CNM): (a) G250 10 mm specimen 01; (b) G250 10 mm specimen 02